COMMUNICATIONS CHEMISTRY

ARTICLE

https://doi.org/10.1038/s42004-019-0236-y OPEN

Isolation and characterisation of a stable 2-azaphenalenyl azomethine ylide

Koji Katayama[1], Akihito Konishi[2,3], Koki Horii[2], Makoto Yasuda[2], Chitoshi Kitamura[4], Jun-ichi Nishida[1] & Takeshi Kawase[1*]

Although azomethine ylides have been fully exploited as versatile reactive intermediates in dipolar cycloaddition reactions to construct a variety of heterocyclic compounds involving a nitrogen atom, little is known about their structural and electronic properties. Here a method is developed for the preparation, isolation and characterization of a stable 2-azaphenalenyl based azomethine ylide. *N*-Phenyl-5,8-di-*t*-butyl-2-azaphenalenyl cannot be isolated because it undergoes rapid dimerization by C–C bond formation at the 1 and 3 positions. In contrast, sterically bulkier *N*-2,6-di(isopropyl)phenyl-5,8-di-*t*-butyl-2-azaphenalenyl can be generated and isolated as deep green crystals under deoxygenated conditions. X-ray crystal analysis of this stable azomethine ylide reveals that its azaphenalenyl skeleton has very small bond alternation and structural deformation. The results of spectroscopic and electrochemical theoretical studies indicate that *N*-2,6-di(isopropyl)phenyl-5,8-di-*t*-butyl-2-azaphenalenyl has electronic features that are similar to those of phenalenyl anion and it possesses an extremely high HOMO energy.

[1] Graduate School of Engineering, University of Hyogo, 2167 Shosha, Himeji, Hyogo 671-2280, Japan. [2] Department of Applied Chemistry, Graduate School of Engineering, Osaka University, 2-1 Yamadaoka, Suita, Osaka 565-0871, Japan. [3] Center for Atomic and Molecular Technologies, Graduate School of Engineering, Osaka University, 2-1 Yamadaoka, Suita, Osaka 565-0871, Japan. [4] School of Engineering, The University of Shiga Prefecture, 2500 Hassaka-Cho, Hikone, Shiga 560-0043, Japan. *email: kawase@eng.u-hyogo.ac.jp

Since the first description in 1862 by Strecker[1], azomethine ylides have been extensively used in organic synthesis as 3-atom, 4π-electron components of 1,3-dipolar cycloaddition reactions with dipolarophiles. Regardless of the fact that the reactivity and methods for generation of these important reactive intermediates have been investigated intensively[2–4], little is known about their detailed structural and electronic properties. Carbonyl-stabilized pyridinium ylide **1** as an azomethine ylide vinylog was synthesized in 1934[3,5]. However, its electronic and structural properties were not elucidated, and it does not have the ability to undergo 1,3-dipolar cycloaddition reactions with dipolarophiles. Azaphenalenes, 14π electron containing isoelectronic analogs of phenalenyl anion **2**, are composed of the four structural isomers displayed in Fig. 1a. The isomers includes 1-azaphenalene **3**[6] and 9b-azaphenalene (cycl[3.3.3]azine) **4**[7], which have been synthesized, and *N*-substituted-2-azaphenalenyl (benzo[*de*]isoquinolinium-1-ide) **5**[8,9] and 9a-azaphenalenyl **6**, which serve as highly reactive azomethine ylides intermediates (Fig. 1b and Supplementary Fig. 1). Dibenzo derivatives of **6**[10–15] were explored earlier by Beljonne, Feng and Müllen, who also reported their absorption spectral properties[10]. *N*-Substituted 2-azaphenalenyl derivatives **5** can be structurally visualized in three resonance forms including azomethine ylide **A**, azaphenalenyl anion **B** and biradical **C** (Fig. 1c).

The effort described here is aimed at the isolation, and structural and electronic characterization of an azomethine ylide. In order to incorporate features that would lead to stabilization of these typically transient species, we design *N*-substituted 2-azaphenalenyl **7a** and **7b**, which contain phenyl and 2,6-di(isopropyl)phenyl groups on nitrogen, as well as bulky *tert*-butyl groups at the 5 and 8 positions. Below, we describe the method employed to isolate the aerobically unstable azomethine ylide **7b** as a green solid and, its structural and electronic characterization.

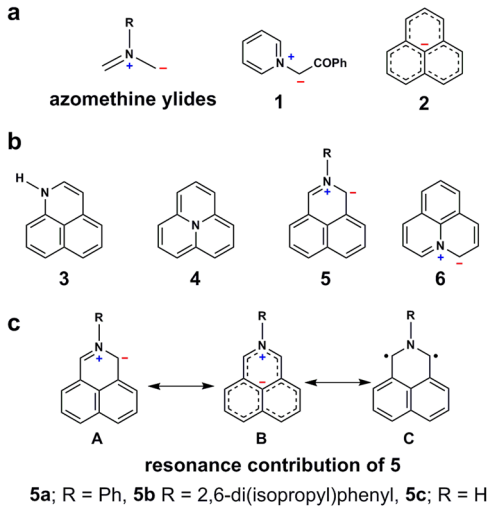

Fig. 1 Structures of azomethine ylides and azaphenalene related compounds. **a** Structures of azomethine ylides, a pyridinium ylide **1** and phenalenyl anion **2**. **b** Structures of 1-azaphenalene **3** and 9b-azaphenalene **4**, and *N*-substituted 2-azaphenalenyl **5a**-**c** and 9a-azaphenalenyl **6**. **c** Resonance contributors of **5**.

Results

Synthesis and reactions. For preparation of the respective *N*-phenyl- and 2,6-di(isopropyl)phenyl-2-azaphenalenyl ylides **7a** and **7b**, we chose to use a protocol involving base induced deprotonation of the corresponding iminium salts **8a** and **8b**. The route began with triphenylcarbenium tetrafluoroborate (Ph_3CBF_4) promoted oxidation of the respective amines **9a** and **9b** (Fig. 2a and Supplementary Fig. 2). Reaction of **8a** with triethylamine (Et_3N) in THF in the presence of *N*-phenyl maleimide (NPMI) produced the dipolar cycloaddition adduct **10** in 66% yield (Fig. 2b). This observation demonstrates that the corresponding azomethine ylide **7a** is generated as a reactive intermediate by Et_3N induced deprotonation of **8a**. Additionally, reaction of **7a** with the as a versatile synthetic intermediate[16–19] *N*-(2-ethylhexyl) acenphthylene-5,6-dicarboxylimide **11** was examined. Under similar conditions, this reaction produces the corresponding cycloadduct **12** in 31% yield (Fig. 2c). Interestingly, treatment of **8a** in the filter paper component of a Soxhlet extractor with hexane-Et_3N vapor led to formation of an amber solid, which upon chromatographic purification produced the colorless dimer initially identified as the dimeric adduct **13** (51%) (Fig. 2d). The results of X-ray crystallographic analysis showed that **13** is comprised of two units of **7a** joined to one another in an anti-manner via C–C bonds at the 1 and 3 positions of each (Fig. 2e, Supplementary Figs. 3 and 4, and Supplementary Table 1).

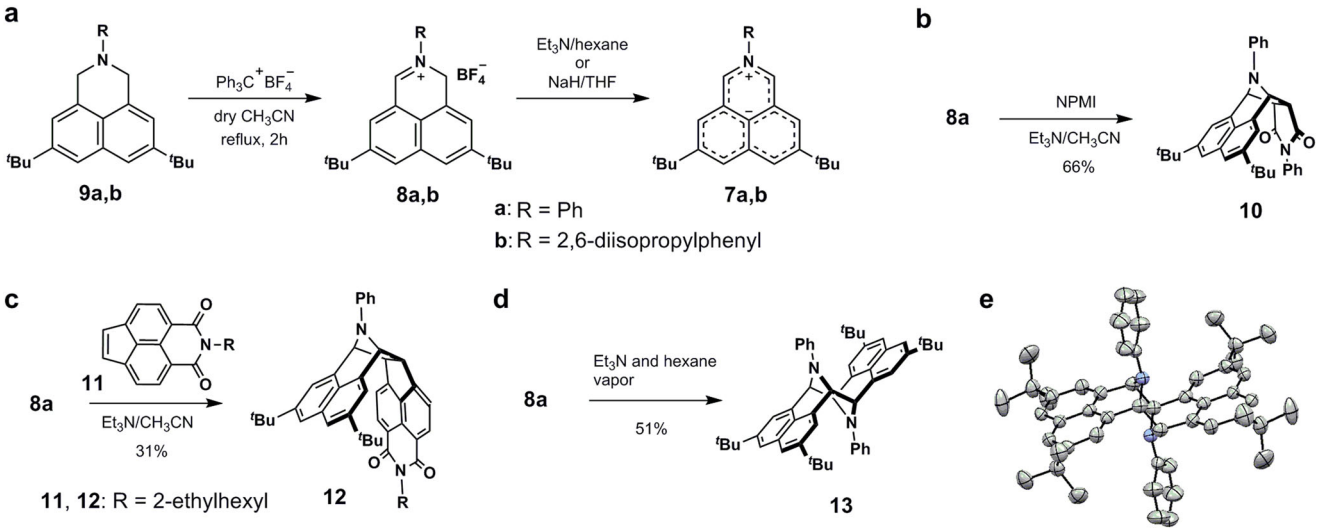

Fig. 2 Preparation of **7a** and **7b** and reactions of **7a**. **a** Synthesis of **7a** and **7b** from **9a** and **9b** via iminium salts **8a** and **8b**. **b** Formation of NPMI adduct **10**. **c** Formation of acenaphthylene imide adduct **12**. **d** Formation of dimer **13**. **e** A crystal structure of **13**.

This unusual dimerization process[20] suggests that **7a** has both biradical and azomethine ylide character. Actually, a theoretical calculation on **5a** at the LC-UBLYP($\mu = 0.33$ bohr^{-1})/6–311 G* level indicated that it has small biradical character ($y = 0.020$) (Supplementary Fig. 5 and Supplementary Table 2). The estimated biradical index of **5a** is small, but it is larger than that of **5b** (R = 2,6-di(isopropyl)phenyl; $y = 0.000$). Thus, it is possible that conjugation of the *N*-phenyl group and main core π-system gives **7a** the biradical character needed to drive the dimerization process.

We believed that it would be possible to prevent this dimerization reaction by replacing the *N*-phenyl group in **7a** with the sterically more bulky 2,6-di(isopropyl)phenyl group. To assess this proposal, iminium salt **8b** was prepared from amine **9b** through Ph_3CBF_4 induced oxidation followed by Et_3N vapor promoted deprotonation in the manner employed to form **7a** (Fig. 2a). This process formed a green solution of the ylide **7b**, which yielded a green solid upon evaporation. Owing to the high reactivity of **7b** with oxygen, the green color of both the solution and solid immediately changed to yellow under aerobic conditions (Supplementary Fig. 6). To avoid this problem and simplify the procedure, we used a method to form **7b** by reaction of iminium salt **8b** with sodium hydride (NaH) in THF in a nitrogen-filled glove box. In this event, ylide **7b** was generated as a green crystalline solid quantitatively.

Absorption spectra. Ylide **7b** was characterized by using UV-vis, FT-IR, ^{1}H-NMR and ^{13}C-NMR spectroscopy, and high resolution mass spectrometry (HRMS), and finally by using X-ray crystallographic analysis. The absorption spectra of **7b** and its precursor **8b** in dichloromethane (DCM) are displayed in Fig. 3. The spectrum of **7b** is comprised of two bands in the 300–450 and 500–800 nm regions, the latter of which has vibronic structure with absorption maxima (λ_{max} (log ε)) values of 614 (2.24), 665 (2.34), and 727 nm (2.19). The results of TD-DFT calculations on the analog **5b** indicate that the 632 nm band corresponds to a HOMO-LUMO transition (Supplementary Fig. 7 and Supplementary Table 3). While **8b** in DCM exhibits intense fluorescence with a maximum (λ_{FL}) at 529 nm and a quantum yield (ϕ) of 0.60 (Supplementary Fig. 8), the corresponding ylide **7b** is non-fluorescent.

Crystallographic analysis and HOMA values. X-ray crystallography was carried out on a single crystal of **7b** (monoclinic $P2_1/c$ space group) obtained using hexane as a solvent. Analysis of the molecular structure shows that the 2-azaphenalenyl system in **7b** possesses a highly planar structure (Fig. 4). The dihedral angle between the azaphenalenyl plane and that of the *N*-aryl ring is 84.7°, indicating that the *N*-phenyl substituent only minimally perturbs the electronic properties of **7b** (Supplementary Figs. 9 and 10, and Supplementary Table 4). The two C-N bond lengths in the crystal structure of **7b** are nearly identical (1.3492(18) and 1.3516(19) Å), and the average (1.350 Å) is comparable to the C–N bonds (1.34 Å) in *N,N'*-dibenzyl-dibenzodiazapyrene dication **14**[21]. While from a structural perspective the C-N-C unit of **7b** is similar to that in the pyridinium ring of **14**, the neighboring NC-C bonds (1.420(2) and 1.421(2) Å) are slightly longer than the corresponding NC-C bonds in **14** (1.39 Å). Moreover, the C-N-C bond angle (123.9(1)°) in **7b** is slightly different than that in a regular hexagon framework because of the shorter nature of C–N vs C-C bonds. All sp^2 carbon bond angles in **7b** are between 117.4° and 123.3° (Supplementary Fig. 10). The harmonic oscillator model of aromaticity (HOMA)[22,23] value of the pyridine ring in **7b** of 0.62 indicates that it has aromatic character (Fig. 4). On the other hand, the benzene rings of the naphthalene moiety in **7b** display a small degree of bond alternation (HOMA = 0.85 and 0.79) and are larger than that of naphthalene itself (0.70)[24].

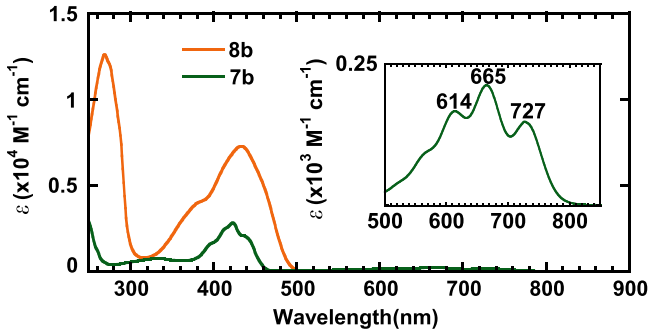

Fig. 3 Absorption spectra of **7b** and **8b**. Absorption spectra of **7b** and **8b** in DCM. Inset: partially enlarged spectrum of **7b** (500 nm to 850 nm).

NMR analysis and NICS(1) values. The ^{1}H- and ^{13}C-NMR spectra of **7b** in THF-d_8 (Supplementary Figs. 11 and 12) contain sharp signals, suggesting that, as is predicted based on theoretical calculations, this substance has negligible biradical character. 2D NMR (HSBC, HSQC and NOESY) spectral analyses enable unambiguous assignment of all protons and carbons in **7b** (Supplementary Figs. 13–16). Selected chemical shift data and nucleus-independent chemical shifts (NICS) (1)[25] values of **7b** together with those of **2**[26,27], **4**[28] and **5b** are listed in Fig. 5. Inspection of the ^{13}C-NMR chemical shifts indicate that the negative charge in **7b** is delocalized over the entire molecule in a manner that is comparable to that in the phenalenyl anion **2**. Theoretical calculations at the GIAO-HF/6–311 + G*//RB3LYP-D3/6–311 G* level indicate that the respective NICS(1) values of the pyridine A and benzene B rings in **5b** are +2.75 and −6.21, indicating that the pyridine ring is slightly paratropic and the benzene rings of the naphthalene moiety are weakly diatropic (Fig. 5). Taking into account the negative charge distribution, the observed chemical shifts suggest that **7b** is a weak diatropic species and, as a result, it can be regarded as a phenalenyl anion perturbed by the presence of a positively charged nitrogen atom.

Electrochemical properties. The electrochemical properties of **7b** were evaluated by using cyclic voltammetry (CV) (Fig. 6 and Supplementary Fig. 17). The CV of **7b** in DCM contains three redox waves associated with irreversible oxidation (+0.56 V), reversible oxidation (−0.68 V) and irreversible reduction (−2.06 V), which correspond to the following transformations: $\mathbf{7b}^{2+} \leftarrow \mathbf{7b}^{\bullet+} \rightleftarrows \mathbf{7b} \rightarrow \mathbf{7b}^{\bullet-}$ (Table 1). The E_1^{ox} value (−0.68 V) is extremely high for a neutral compound especially when considering the fact that the typical electron donor tetrathiafulvalene (TTF)[29] has an oxidation potential of +0.37 V. Moreover, the high E_1^{ox} value of **7b** explains its high reactivity toward oxygen. Finally, the HOMO-LUMO energy gap, estimated using redox potential data) is comparable to that of absorption edge of **7b** (1.51 eV/823 nm) (Supplementary Fig. 7).

Discussion

In the effort described above, *N*-phenyl- and *N*-2,6-di(isopropyl) phenyl-2-azaphenalenyl, **7a** and **7b**, were generated from the corresponding iminium ions **8a** and **8b** by treatment with gaseous Et_3N. The phenyl derivative **7a** is a highly reactive species that, in the absence of a dipolarophile, undergoes ready dimerization by C–C bond formation at the 1 and 3 positions. This finding is in good accord with the results of theoretical calculations that indicate that **5a** possesses slight biradical character. In contrast, **7b** containing a bulky *N*-substituent is more stable and can be

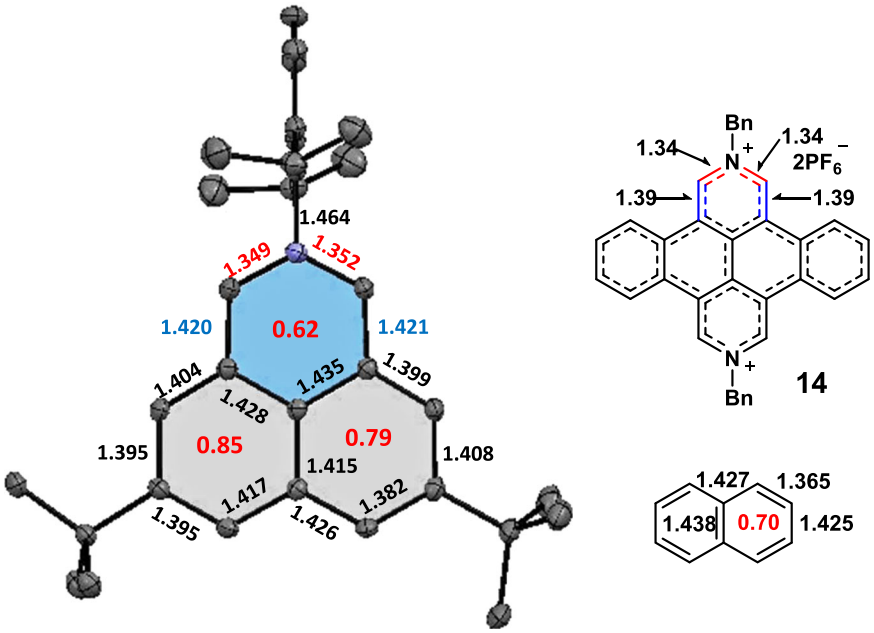

Fig. 4 Structure of **7b**. Molecular structures, bond lengths and HOMA values of **7b** and the related compounds.

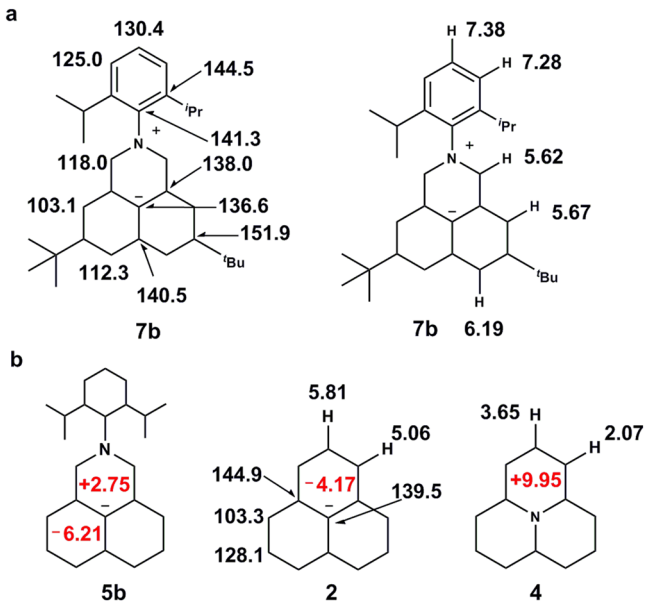

Fig. 5 NMR assignments and NICS(1) values of **7b** and related compounds. **a** Partial ^{1}H- and ^{13}C-NMR assignments of **7b**. **b** ^{1}H- and ^{13}C-NMR assignments of **2** and **4**, and the NICS(1) values (red letters) of **2**, **4**, and **5b** were calculated at the GIAO-HF/6-311 + G*//RB3LYP-D3/6-311 G* level.

isolated under anaerobic conditions. Because the use of substituents for further electronic stabilization could result in loss of azomethine ylide features, like that occurring with **1**, **7b** should be a good model for elucidation of the electronic and structural features of azomethine ylides. X-ray analysis of **7b** reveals that the structural features corresponding to the azomethine ylide unit are similar to those of the corresponding region of diazapyrene dication **14**. The characteristics of **7b**, evaluated by using spectroscopy, indicate that it has electronic features that are similar to those of phenalenyl anion **2**. The results of HOMA and NICS(1) calculations also support this conclusion. Finally, the high reactivity of **7b** with molecular oxygen is a consequence of its high oxidation potential associated with a HOMO energy.

The results described above open the way for construction of new compounds bearing the *N*-substituted 2-azaphenalenyl core structure. For example, it is possible that appropriate functionalization can be used to tune the electronic properties of the 2-azaphenalenyl system and to produce electron donor systems with high thermal stabilities. Moreover, transition metal complexes comprised of *N*-substituted 2-azaphenalenyl ligands would be intriguing from both physicochemical and synthetic points of view[30].

Methods

General. All reactions of air- or moisture-sensitive compounds were carried out in a dry vessel under a positive pressure of nitrogen. Air- and moisture-sensitive liquids and solutions were transferred *via* syringe. Analytical thin-layer chromatography was performed using glass plates pre-coated with Merck Art. 7730 Kieselgel 60 GF-254. Thin layer chromatography plates were visualized by exposure to UV light. Organic solutions were concentrated by using rotary evaporation at *ca.* 15 Torr obtained with a diaphragm pump. Column chromatography was performed with Merck Kiesel-gel 60. All reagents were commercially available and used without further purification unless otherwise noted. THF was purchased from Wako Chemical Co. and distilled from lithium aluminum hydride at 760 Torr under a nitrogen atmosphere before use.

Melting points were recorded on a Yanaco MP–S3 apparatus and reported uncorrected. Positive FAB and EI mass spectra were recorded on a JEOL JMS-700 and a Shimadzu GCMS-QP2010 Ultra, respectively. High-resolution mass spectra were obtained using an Applied Biosystem Japan Ltd. ^{1}H and ^{13}C NMR spectra of all compounds except **7b** and **12** were recorded using a Bruker-Biospin DRX-500 spectrometer. The NMR spectral data were measured at 20 °C. IR spectra of all compounds except **7b** and **12** were obtained using a Shimadzu FTIR-8400 spectrometer. NMR spectra of **7b** and **12** were recorded using JEOL-AL400 (400 MHz for ^{1}H, and 100 MHz for ^{13}C) and Bruker AVANCE III spectrometers (600 MHz for ^{1}H, and 150 MHz for ^{13}C) with TMS as an internal standard. ^{19}F and ^{11}B NMR spectra of **8a** and **8b** were recorded using a JEOL-AL400 spectrometer (126.9 MHz for ^{11}B, and 372.4 MHz for ^{19}F) with BF_3 Et_2O as an external standard. UV–vis and fluorescence spectra of **8a** and **8b** in DCM were recorded using a JASCO V650 and a SHIMADZU RF-5300PC spectrophotometer, respectively. Quantum yields for solution state fluorescence (Φ_{SN}) of **8a** and **8b** were determined using 9,10-diphenylanthracene ($\Phi_{SN} = 0.86$)[31] in DCM as an actinometer. ^{1}H and ^{13}C NMR resonances of **7b** were assigned using HSQC, HSBC, NOESY, and ^{13}C off-resonance techniques. UV-vis-NIR spectra of **7b** and **12** were recorded using a SHIMAZU UV-3600 spectrophotometer. The IR spectrum of **7b** and **12** was recorded as a solid in a KBr pellet using a JASCO FT/IR 6200 spectrophotometer. Cyclic voltammetric measurements of **7b** was performed using an ALS-600C electrochemical analyzer with a glassy carbon working, Pt counter, and $Ag/AgNO_3$ reference electrodes at room temperature in DCM containing 0.1 M Bu_4NClO_4 as the supporting electrolyte. DFT calculations were carried out using the Gaussian 09 program package[32].

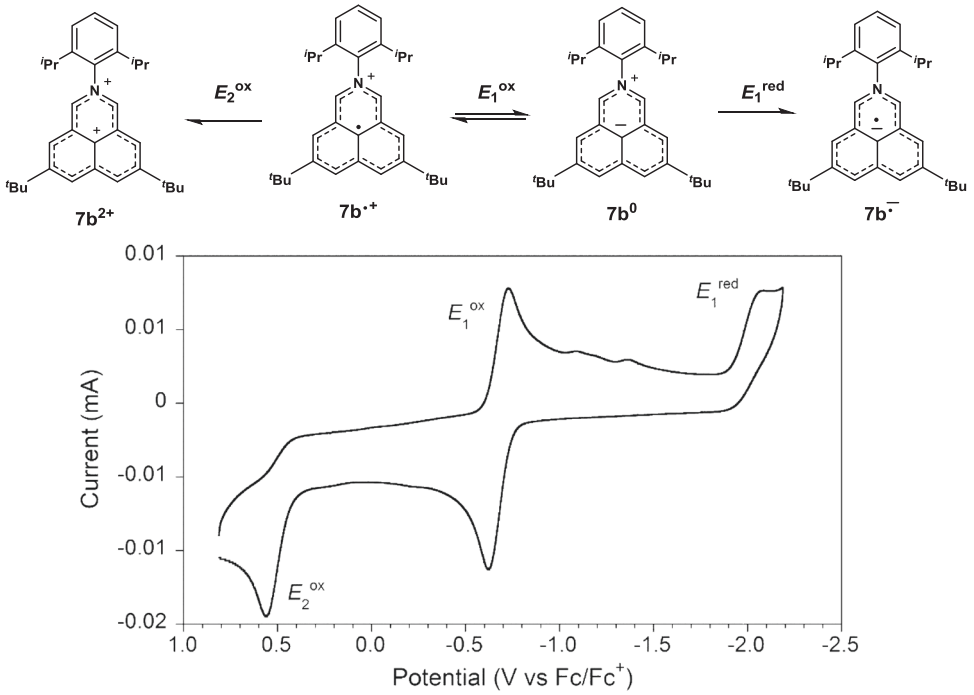

Fig. 6 Electrochemical analysis. Cyclic voltammogram of **7b** (vs. Ag/Ag^+, in 0.1 M nBu_4NClO_4/DCM, scan rate 0.1 V/s, 25 °C, $Fc/Fc^+ = 0$ V), and theoretical energy diagram of **5b**. (Fc = ferrocene).

Table 1 Redox properties in DCM and frontier orbital energies of 7b.

E_2^{ox}	E_1^{ox}	E_2^{red}	E_{gap} [b]	LUMO[c]	HOMO[d]	E_{gap}[e]/λ_{onset}
+0.56[a]	−0.68	−2.06[a]	1.41 eV	−2.71 eV	−4.12 eV	1.51 eV/823 nm

[a] Peak potential. [b] $E_{gap} = E_1^{ox} - E_1^{red}$. [c] $E_{LUMO} = -4.8$ eV $- E_1^{red}$. [d] $E_{HOMO} = -4.8$ eV $- E_1^{ox}$. [e] $E_{gap} = 1240/\lambda_{onset}$.

Synthesis of 9a and 9b. The naphthopiperidine derivative **9a** and **9b** were synthesized starting with 3,6-di-*tert*-butyl-1,8-naphthalenedicarboxylic acid anhydride[33] through sequential reduction with lithium aluminum hydride, bromination with boron tribromide, and respective reactions with aniline and 2,6-diisopropylaniline. Full synthetic details are given in the Supplementary Methods.

***N*-Phenyl-5,8-di-*tert*-butyl-1*H*-benz[*de*]isoquinolinium tetrafluoroborate 8a**. A mixture of **9a** (0.10 g, 0.29 mmol) and Ph_3CBF_4 (0.10 g, 0.36 mmol) in dry-acetonitrile (2 mL) was stirred at reflux for 2 h. After cooling to rt, the mixture was diluted with diethyl ether (Et_2O) to afford **8a** (0.11 g, 0.26 mmol) as an orange precipitate in 94% yield. Decomp. 242−243 °C; ^1H NMR (500 MHz, $CDCl_3$): δ 9.45 (s, 1 H), 8.49 (s, 1 H), 8.15 (s, 1 H), 7.80 (m, $J_{o,m} = 8.0$ Hz, 2 H, *o*-H of Ph), 7.77 (s, 1 H), 7.61 (s, 1 H), 7.55 (m, $J_{o,p} = 7.7$ Hz, 2 H, *m*-H of Ph), 7.48 (m, $J_{m,p} = 7.4$ Hz, 1 H, *p*-H of Ph), 5.92 (s, 2 H), 1.45 (s, 9 H), 1.41 (s, 9 H); ^{13}C NMR (126 MHz, $CDCl_3$) δ 166.7, 152.4, 151.5, 141.9, 137.7, 135.6, 132.2, 131.6, 130.7, 124.3, 124.1, 123.1, 122.1, 121.8, 56.0, 35.31, 35.28, 31.1, 30.8 ppm; $^{11}B\{^1H\}$ NMR (127 MHz, $CDCl_3$) δ −0.90 ppm; ^{19}F NMR (372 MHz, $CDCl_3$) δ 1.70 ppm; IR (KBr): ν 2956 (s), 2908 (m), 2871 (m), 1635 (m), 1608 (m), 1581 (m), 1524 (m), 1469 (m), 1377 (m), 1243 (m), 1083 (s), 758 (m) cm^{-1}; UV/Vis (DCM): λ_{max} (log ε) 287 (3.90), 437 (3.83) nm; FL (DCM): λ_{FL} 555 nm ($\Phi_{SN} = 0.11$); HRMS (FAB, NBA) m/z: calcd. for $[C_{26}H_{30}N^+]$: 356.2373; found: 356.2377.

***N*-2,6-Di(isopropyl)phenyl-5,8-di-*tert*-butyl-1*H*-benz[*de*]isoquinolinium tetrafluoroborate 8b**. A mixture of **9b** (0.11 g, 0.24 mmol) and Ph_3CBF_4 (0.093 g, 0.28 mmol) in dry-acetonitrile (2 mL) was stirred at reflux for 2 h. After cooling to rt, the mixture was concentrated in vacuo. The resulting solid was dissolved in ethyl acetate and diluted with hexane to afford **8b** (0.114 g, 0.22 mmol) a yellow precipitate in 90% yield. Decomp. 239−240 °C; ^1H NMR (500 MHz, $CDCl_3$): δ 9.47 (s, 1 H), 8.73 (s, 1 H), 8.20 (s, 1 H), 7.83 (s, 1 H), 7.56 (t, $J = 7.6$ Hz, 1 H), 7.55 (s, 1 H), 7.37 (d, $J = 7.9$ Hz, 2 H), 5.55 (s, 1 H), 2.94 (sep, $J = 6.5$ Hz, 2 H), 1.47 (s, 9 H), 1.42 (s, 9 H), 1.34 (d, $J = 6.5$ Hz, 6 H), 1.32 (d, $J = 6.5$ Hz, 6 H); ^{13}C NMR (126 MHz, $CDCl_3$) δ 171.2, 152.4, 152.1, 142.9, 138.9, 137.4, 135.8, 132.4, 131.9, 128.3, 125.7, 123.7, 123.6, 122.1, 120.9, 58.6, 35.4, 35.3, 31.1, 30.8, 28.9, 24.7, 24.2 ppm; $^{11}B\{^1H\}$ NMR (127 MHz, $CDCl_3$) δ −0.99 ppm; ^{19}F NMR (372 MHz, $CDCl_3$) δ 1.93 ppm; IR (KBr): ν 2959 (s), 2870 (m), 1644 (m), 1614 (m), 1520 (m), 1464 (m), 1377 (m), 1281 (m), 1241 (m), 1218 (m), 1185 (m), 1047 (s) cm^{-1}; UV/Vis (DCM): λ_{max} (log ε) 269 (4.10), 433 (3.86) nm; FL (DCM): λ_{FL} 529 nm ($\Phi_{SN} = 0.60$); HRMS (FAB, NBA) m/z: calcd. for $[C_{32}H_{42}N^+]$: 440.3312; found: 440.3319.

***N*-Phenylmaleimide adduct 10**. A mixture of **8a** (100 mg, 0.30 mmol), Et_3N (0.15 mL, 1.1 mmol) and NPMI (66 mg, 0.38 mmol) in dry-acetonitrile (3 mL) was stirred at reflux under N_2 for overnight. Concentration in vácuo gave a residue that was subjected to column chromatography on silica gel (elution with 2:1 DCM:ethyl acetate) to afford **10** (54 mg, 0.13 mmol) as a colorless solid in 66% yield. M.p. 249−250 °C; ^1H NMR (500 MHz, $CDCl_3$): δ 7.54 (d, $J = 1.7$ Hz, 2 H), 7.43 (d, $J = 1.7$ Hz, 2 H), 7.17–7.08 (m, 5 H), 6.90 (d, $J = 7.9$ Hz, 2 H), 6.69 (t, $J = 7.3$ Hz, 1 H), 5.98 (dd, $J = 8.2$, 1.3 Hz, 2 H), 5.64 (dd, $J = 5.3$, 2.4 Hz, 2 H), 4.26 (dd, $J = 5.3$, 2.4 Hz, 2 H), 1.33 (s, 18 H); ^{13}C NMR (126 MHz, $CDCl_3$) δ 174.0, 148.8, 146.0, 133.0, 131.2, 130.3, 129.1, 128.7, 128.4, 126.2, 123.9, 123.5, 122.3, 119.6, 116.8, 62.7, 53.1, 34.8, 31.1 ppm; IR (KBr): ν 2952 (m), 2922 (m), 2854 (m), 1710 (m), 1695 (s), 1655 (s), 1435 (m), 1412 (m), 1335 (m), 1235 (m), 1078 (m), 756 (m), 698 (m) cm^{-1}; HRMS (EI) m/z: calcd. for $[C_{36}H_{36}N_2O_2]$: 528.2777; found: 528.2780.

***N*-(2-Ethylhexyl)acenphthylene-5,6-dicarboxylimide adduct 12**. A mixture of **8a** (103 mg, 0.232 mmol), Et_3N (0.1 mL, 0.721 mmol) and *N*-(2-ethylhexyl) acenphthylene-5,6-dicarboxylimide **11** (112 mg, 0.336 mmol) in dry-acetonitrile (10 mL) was stirred at reflux under N_2 for overnight. Concentration in vácuo gave a residue that was subjected to column chromatography on silica gel (elution with chloroform) to afford **12** (50.2 mg, 0.073 mmol) as a yellow solid in 31% yield. M.p. 152−153 °C; ^1H NMR (400 MHz, $CDCl_3$) δ 8.14 (dd, $J = 7.4$, 1.4 Hz, 2 H), 7.30 (dd, $J = 7.6$, 2.0 Hz, 2 H), 7.26–7.07 (m, 4 H), 7.01–6.97 (m, 4 H), 6.66 (t, $J = 7.2$ Hz, 1 H), 5.74 (dd, $J = 5.4$, 2.2 Hz, 2 H), 5.18 (dd, $J = 6.0$, 1.6 Hz, 2 H), 4.00–3.91 (m, 2 H), 1.83–1.77 (m, 1 H), 1.36–1.20 (m, 26 H), 0.88–0.81 (m, 6 H) ppm; ^{13}C NMR (100 MHz, $CDCl_3$) δ 164.44, 164.40, 150.5, 147.7, 147.3, 138.8, 132.7, 132.6, 132.5, 131.5, 129.0, 125.5, 123.9, 122.6, 122.4, 120.9, 119.38, 119.35, 119.0, 116.7, 63.4, 58.3, 43.9, 37.9, 34.5, 30.9, 30.7, 28.7, 24.1, 23.0, 14.0, 10.6 ppm; IR (KBr): ν 2960 (m), 1699 (s), 1662 (s), 1626 (s), 1598 (m), 1497 (m), 1456 (m), 1419 (m), 1335

(m), 1235 (m), 758 (m), 462 (m), 418 (m) cm^{-1}; UV/Vis (DCM): λ_{max} (log ε) 378 (4.12), 359 (4.24), 345 (4.16), 234 (4.00); FL (DCM): λ_{FL} 686 nm ($\Phi_{SN} < 0.01$); MS (CI^+, 70 eV) m/z 689 ($[M + H]^+$, 100), 358 (22), 336 (43); HRMS (CI^+, 70 eV) Calculated ($C_{48}H_{53}N_2O_2$) 689.4107 ($[M + H]^+$), Found: 689.4118.

***N*-Phenyl-2-azaphenalenyl dimer 13**. A Soxhlet extractor was equipped with a reflux condensor and a 50 mL of flask containing with Et_3N (5 mL) and hexane (35 mL). The filter paper for the Soxhlet exstractor was charged with **8a** (500 mg, 1.1 mmol) and placed in the apparatus, and purged with N_2 gas. The flask was heated to bring about reflux for 2 h. Then, brown solids was formed on the filter paper. The brown solid formed on the filter paper was removed by dissolving in cyclohexane. The cyclohexane solution was concentrated in vácuo to give dimer **13** (206 mg, 0.29 mmol) as a colorless solid in 51% yield. M.p. > 300 °C; ^1H NMR (500 MHz, $CDCl_3$): δ 7.60 (s, 4 H), 7.60 (s, 2 H), 6.83 (m, 4 H, *m*-H of Ph), 6.45 (m, 6 H, *o,p*-H of Ph), 5.06 (s, 4 H), 1.47 (s, 36 H); ^{13}C NMR (126 MHz, $CDCl_3$) δ 150.1, 148.2, 133.4, 132.3, 128.5, 126.9, 122.2, 120.2, 118.5, 116.4, 63.8, 34.9, 31.5 ppm; IR (KBr): ν 2961 (s), 2360 (m), 1633 (m), 1594 (m), 1496 (m), 1397 (m), 1369 (m), 1243 (m), 1060 (m), 757 (m) cm^{-1}; UV/Vis (DCM): λ_{max} (log ε) 260 (4.12), 295 (3.89) nm; HRMS (EI) m/z: calcd. for $[C_{52}H_{58}N_2]$: 710.4600; found: 710.4608.

***N*-2,6-Di(isopropyl)phenyl-5,8-di-*tert*-butyl-2-azaphenalenyl 7b**. In a glove box filled with N_2, a solution of **8b** (55 mg, 0.11 mmol) and NaH (97 mg, 4.0 mmol) in THF (4 mL) was stirred at rt for 3 h. Filtration of the mixture gave a filtrate that was concentrated in vácuo to afford **7b** as a green solid (46 mg, 0.11 mmol). According to the NMR monitoring (in THF-d_8), **7b** was generated quantitatively. Decomp. 101 −102 °C; ^1H NMR (600 MHz, THF-d_8): δ 7.38 (t, $J = 7.8$ Hz, 1 H, H-11), 7.28 (d, $J = 7.8$ Hz, 2 H, H-10), 6.19 (d, $J = 1.8$ Hz, 2 H, H-5), 5.67 (d, $J = 1.8$ Hz, 2 H, H-3), 5.62 (s, 2 H, H-1), 3.55 (sep, $J = 7.2$ Hz, 2 H, H-13), 1.30 (d, $J = 7.2$ Hz, 12 H, H-12), 1.15 (s, 18 H, H-14); ^{13}C NMR (150 MHz, THF-d_8, rt) δ 151.9 (s, C-4), 144.5 (s, C-9), 141.3 (s, C-8), 140.5 (s, C-6), 138.0 (s, C-2), 136.6 (s, C-7), 130.4 (d, C-11), 125.0 (d, C-10), 118.0 (d, C-1), 112.3 (d, C-5), 103.1 (d, C-3), 34.6 (s, C-15), 31.2 (q, C-14), 28.8 (d, C-13), 25.0 (q, C-12) ppm; IR (KBr): ν 2962 (s), 2867 (m), 1610 (s), 1568 (s), 1459 (m), 1423 (m), 1361 (s), 1332 (m), 1279 (m), 851 (m), 802 (m), 764 (m) cm^{-1}; UV/Vis (DCM): λ_{max} (log ε) 332 (2.87), 423 (3.45), 614 (2.24), 665 (2.34), 727 (2.19) nm; HRMS (EI) m/z: calcd. for $[C_{32}H_{41}N]$: 439.3239; found: 439.3238.

^1H, ^{11}B, ^{19}F and ^{13}C NMR, and Mass spectra of new compounds. See Supplementary Figs. 11–16 and 18–31.

Mass spectra of new compounds. See Supplementary Figs. 32–41.

X-ray diffraction analysis. Single crystals of **7b** for X-ray analysis were obtained by slow evaporation from an *n*-hexane solution. X-ray diffraction data were collected on a Rigaku XtaLAB Synergy-S diffractometer equipped with HyPix-6000HE Hybrid Photon Counting (HPC) X-ray detector with graphite-monochromated MoKα ($\lambda = 0.71073$ Å) radiation, and Φ and ω scans at a maximum 2θ value of 61.8. The crystal was kept at 123 K during data collection. Using Olex2[34], the structure was solved with the ShelXT[35] structure solution program using Intrinsic Phasing and refined with the ShelXL[36] refinement package using Least Squares minimization.

A single crystal of **13** for X-ray analysis was obtained by slow evaporation from a toluene solution. X-ray diffraction data were collected on a Rigaku Rapid Auto diffractometer with graphite-monochromated MoKα ($\lambda = 0.71075$ Å) radiation, and Φ and ω scans at a maximum 2θ value of 50.7°. The structures were solved by a direct method using SHELXL Version 2018/3[37]. All non-hydrogen atoms were refined anisotropically by full-matrix least-squares on F^2 using SHELXT version 2018/2[38]. Hydrogen atoms of **13** were refined using the riding model. All calculations were performed using the CrystalStructure crystallographic software package[39] except for refinement, which was performed using SHELXL Version 2018/3. Crystallographic details are given in CIF files (Supplementary Data 1 and 2). The detailed crystallographic data for both the compounds are listed in Supplementary Tables 1 and 4.

HOMA calculations. HOMA values of **7b** and naphthalene were calculated using C–C and C–N bond lengths derived from the X-ray crystallographic structure, according to the following equation $HOMA = 1 - \alpha/n\Sigma(R_{opt} - R_i)^2$, where n is the number of bonds taken in the summation, α is an empirical constant, R_{opt} is an optimal bond length and R_i is a bond length of ith bond. R_{opt}.1.388 (C–C) and 1.334 (C–N) Å and $\alpha = 257.7$ (C–C) and 93.52 (C–N) were used[22].

Theoretical calculations. All calculations were conducted using the Gaussian 09 program[32]. The geometries of **2**, **3**, **4**, **5a**–**c**, and naphthalene were optimized with the RB3LYP-D3 functional and 6–311 G* basis set. The optimized geometries were used for calculations of the other properties. The values of y of **5a** and **5b** were obtained from the occupation number of the lowest unoccupied natural orbital (LUNO) ($y = n_L$) at the LC-UBLYP($\mu = 0.33$ $bohr^{-1}$)/6–311 G* level. The NICS(1) values of **2**, **3**, **5a**, **5b**, and naphthalene were calculated at the GIAO-HF/6–311 + G* level. Electronic excitation properties of **5b** were evaluated by using the TD-DFT method RB3LYP and 6–311 + G* basis set.

Data availability

Data for the crystal structures reported in this paper have been deposited at the Cambridge Crystallographic Data Centre (CCDC) under the deposition numbers CCDC 1950740 (**7b**) and 1950741 (**13**). Copies of these data can be obtained free of charge via www.ccdc.cam.ac.uk/data_rquest/cif. All other data generated during this study are available from the corresponding author on request.

Received: 29 May 2019; Accepted: 29 October 2019;
Published online: 29 November 2019

References

1. Strecker, A. On a peculiar oxidation by alloxan. *Justus Liebigs Ann. Chem.* **123**, 363–365 (1862).
2. Coldham, I. & Hufton, R. Intramolecular dipolar cycloaddition reactions of azomethine ylides. *Chem. Rev.* **105**, 2765–2809 (2005).
3. Pinho e Melo, T. M. V. D. Conjugated Azomethine Ylides. *Eur. J. Org. Chem.* **2006**, 2873–2888 (2006).
4. Tang, S., Zhang, X., Sun, J., Niu, D. & Chruma, J. J. 2-Azaallyl anions, 2-azaallyl cations, 2-azaallyl radicals, and azomethine ylides. *Chem. Rev.* **118**, 10393–10457 (2018).
5. Kröhnke, F. Synthesen mit Hilfe von Pyridiniumsalzen. *Angew. Chem.* **65**, 605–627 (1953).
6. O'Brien, S. & Smith, D. C. C. The synthesis of heterocyclic analogues of phenalene (perinaphthene), containing one hetero-atom. *J. Chem. Soc.* 2907–2917 (1963).
7. Farquhar, D. & Leaver D. Synthesis of pyrido[2,1,6-*de*]quinolizine (cycl[3,3,3] azine). *J. Chem. Soc. D.* **1969**, 24-25 (1969).
8. Sha, C.-K. & Wang, D.-C. Synthesis of the parent compound and *N*-substituted derivatives of 1*H*-benz[*de*]isoquinoline and benzo[*de*] isoquinolinium-1-ide. *Tetrahedron* **50**, 7495–7502 (1994).
9. Zheng, S., Lan, J., Khan, S. I. & Rubin, Y. Synthesis, characterization, and coordination chemistry of the 2-azaphenalenyl radical. *J. Am. Chem. Soc.* **125**, 5786–5791 (2003).
10. Berger, R. et al. Synthesis of nitrogen-doped zigzag-edge peripheries: dibenzo-9*a*-azaphenalene as repeating unit. *Angew. Chem. Int. Ed.* **53**, 10520–10524 (2014).
11. Berger, R., Wagner, M., Feng, X. & Müllen, K. Polycyclic aromatic azomethine ylides: a unique entry to extended polycyclic heteroaromatics. *Chem. Sci.* **6**, 436–441 (2015).
12. Ito, S., Tokimaru, Y. & Nozaki, K. Isoquinolino[4,3,2-*de*]phenanthridine: synthesis and its use in 1,3-dipolar cycloadditions to form nitrogen-containing polyaromatic hydrocarbons. *Chem. Commun.* **51**, 221–224 (2015).
13. Tokimaru, Y., Ito, S. & Nozaki, K. A hybrid of corannulene and azacorannulene: synthesis of a highly curved nitrogen-containing buckybowl. *Angew. Chem. Int. Ed.* **57**, 9818–9822 (2018).
14. Tokimaru, Y., Ito, S. & Nozaki, K. Synthesis of pyrrole-fused corannulenes: 1,3-dipolar cycloaddition of azomethine ylides to Corannulene. *Angew. Chem. Int. Ed.* **57**, 15560–15564 (2018).
15. Arikawa, S., Shimizu, A. & Shintani, R. Azoniadibenzo[*a,j*]phenalenide: A polycyclic zwitterion with singlet biradical character. *Angew. Chem. Int. Ed.* **58**, 6415–6419 (2019).
16. Kawajiri, I. et al. π-Extended fluoranthene imide derivatives: synthesis, structures, and electronic and optical properties. *Can. J. Chem.* **95**, 371–380 (2017).
17. Yamamoto, Y. et al. Synthesis and properties of a decacyclene monoimide and a naphthalimide derivative as three-dimensional acceptor-donor-acceptor system. *Chem. Asian J.* **13**, 790–798 (2018).
18. Ishikawa, H., Katayama, K., Nishida, J., Kitamura, C. & Kawase, T. Fluoranthene and its π-extended diimides: construction of new electron acceptors. *Tetrahedron Lett.* **59**, 3782–3786 (2018).
19. Katayama, K., Kawajiri, I., Okano, Y., Nishida, J. & Kawase, T. Highly polarized benzo[*k*]fluoranthene imide derivatives: displaying large solvatofluorochromism, dual fluorescence and aggregation induced emission associated with excited-state intramolecular charge transfer. *ChemPlusChem* **84**, 722–729 (2019).
20. Guerra, P. V. & Yaylayan, V. Dimerization of azomethine ylides: An alternate route to pyrazine formation in the Maillard reaction. *J. Agric. Food Chem.* **58**, 12523–12529 (2010).
21. Yang, Y. et al. Facile Synthesis of π-extended viologens: electron-deficient polycyclic aza-aromatics. *Chem. Eur. J.* **23**, 7409–7413 (2017).

22. Krygowski, T. M. Crystallographic studies of inter- and intramolecular interactions reflected in aromatic character of π-electron systems. *J. Chem. Inf. Compt. Sci.* **33**, 70–78 (1993).
23. Zborowski, K. K., Alkorta, I., Elguero, J. & Proniewicz, L. M. Calculation of the HOMA model parameters for the carbon-boron bond. *Struct. Chem.* **23**, 595–600 (2012).
24. Cruickshank, D. W. J. A detailed refinement of the crystal and molecular structure of naphthalene. *Acta Crystllogr* **10**, 504–508 (1957).
25. Chen, Z. et al. Nucleus-independent chemical shifts (NICS) as an aromaticity criterion. *Chem. Rev.* **105**, 3842–3888 (2005).
26. Sethson, I., Johnels, D., Edlund, U. & Sygula, A. Electronic and ring current structure of phenalenyl Ions. *J. Chem. Soc. Perkin Trans.* **2**, 1339–1341 (1990).
27. Hempenius, M. A. et al. Spectrometry and reactivity of phenalenyl anions. *J. Phys. Org. Chem.* **7**, 296–302 (1994).
28. Farquhar, D., Gough, T. T. & Leaver, D. Heterocyclic compounds with bridgehead nitrogen atoms. Part V. Pyrido[2,1,6-*de*]quinolizines (cycl[3.3.3] azines). *J. Chem. Soc. Perkin Trans.* **1**, 341–355 (1976).
29. Schröder, H. V. & Schalley, C. A. Tetrathiafulvalene – a redox-switchable building block to control motion in mechanically interlocked molecules. *Beilstein J. Org. Chem.* **14**, 2163–2185 (2018).
30. Nakasuji, K., Yamaguchi, M. & Murata, I. First realization of threefold fluxionality in polycyclic conjugated hydrocarbon-metal complexes: synthesis and dynamic NMR study of [Pd(η^3-phenalenyl)(tmeda)]$^+PF_6^-$ and its methyl derivative. *J. Am. Chem. Soc.* **108**, 325–3327 (1986).
31. Morris, J. V., Mahaney, M. A. & Huber, J. R. Fluorescence quantum yield determinations. 9,10-Diphenylanthracene as a reference standard in different solvents. *J. Phys. Chem.* **80**, 969–974 (1976).
32. Frisch, M. J. et al. *Gaussian 09, Revision D.01*. (Gaussian, Inc., Wallingford, CT, 2013).
33. Altieri, A. et al. Electrochemically switchable hydrogen-bonded molecular shuttles. *J. Am. Chem. Soc.* **125**, 8644–8654 (2003).
34. Dolomanov, O. V., Bourhis, L. J., Gildea, R. J., Howard, J. A. K. & Puschmann, H. OLEX2: a complete structure solution, refinement and analysis program. *J. Appl. Crystallogr* **42**, 339–341 (2009).
35. Sheldrick, G. M. SHELXT – Integrated space-group and crystal-structure determination. *Acta Crystallogr. Sect. A Found. Adv.* **71**, 3–8 (2015).
36. Sheldrick, G. M. Crystal structure refinement with SHELXL. *Acta Crystallogr. Sect. C. Struct. Chem.* **71**, 3–8 (2015).
37. Sheldrick, G. M. A short history of SHELX. *Acta Crystallogr. Sect. A Found. Crystallogr.* **64**, 112–122 (2008).
38. Sheldrick, G. M. Integrating space group determination and structure solution. *Acta Cryst.* **A70**, C1437 (2014).
39. CrystalStructure 4.3: Crystal Structure Analysis Package, Rigaku Corporation (2000–2018). Tokyo 196-8666, Japan.

Acknowledgements

We thank Dr. Hiroyasu Sato (Rigaku Corporation) for assistance with the X-ray analysis of the dimer **13**. This study was financially supported by Hyogo prefecture and a JSPS Grant-in-Aid for Scientific Research (C) (JP16K05896, JP18K05091).

Author contributions

T.K. conceived the project, designed molecules, interpreted the results and drafted the paper. K.K. synthesized all compounds, conducted the UV/vis absorption, fluorescence, IR spectroscopy and Cyclic Voltammetry studies, and carried out detailed DFT and TD-DFT calculations, under the supervision of T.K. J.N. assisted K.K. C.K. determined the crystal structure of **13**. A.K. determined the crystal structure of **7b**, performed mass spectrometric analysis of all compounds, and conducted detailed DFT and TD-DFT calculations on **2**, **4**, **5a**–**c**, **7a** and **7b**. K.H. performed NMR measurements and chemical shift assignments of **7b** and **12**, and performed ^{11}B- and ^{19}F-NMR measurements on **8a** and **8b**. A.K. and K.H. were supervised by M.Y.

Competing interests

The authors declare no competing interests.

Additional information

Supplementary information is available for this paper at https://doi.org/10.1038/s42004-019-0236-y.

Correspondence and requests for materials should be addressed to T.K.

Reprints and permission information is available at http://www.nature.com/reprints

Publisher's note Springer Nature remains neutral with regard to jurisdictional claims in published maps and institutional affiliations.